scientific reports

Check for updates

OPEN

Towards understanding climate change impacts: monitoring the vegetation dynamics of terrestrial national parks in Indonesia

Fatwa Ramdani[1,2]✉, Putri Setiani[3] & Riswan Sianturi[4]

Monitoring vegetation dynamics in terrestrial national parks (TNPs) is crucial for ensuring sustainable environmental management and mitigating the potential negative impacts of short- and long-term disturbances understanding the effect of climate change within natural and protected areas. This study aims to monitor the vegetation dynamics of TNPs in Indonesia by first categorizing them into the regions of Sumatra, Jawa, Kalimantan, Sulawesi, and Eastern Indonesia and then applying ready-to-use MODIS EVI time-series imageries (MOD13Q1) taken from 2000 to 2022 on the GEE cloud-computing platform. Specifically, this research investigates the greening and browning fraction trends using Sen's slope, considers seasonality by analyzing the maximum and minimum EVI values, and assesses anomalous years by comparing the annual time series and long-term median EVI value. The findings reveal significantly increasing greening trends in most TNPs, except Danau Sentarum, from 2000 to 2022. The seasonality analysis shows that most TNPs exhibit peak and trough greenness at the end of the rainy and dry seasons, respectively, as the vegetation response to precipitation increases and decreases. Anomalies in seasonality that is affected by climate change was detected in all of the regions. To increase TNPs resilience, suggested measures include active reforestation and implementation of Assisted Natural Regeneration, strengthen the enforcement of fundamental managerial task, and forest fire management.

Keywords Vegetation dynamics, MOD13Q1, Terrestrial national parks, Indonesia, Enhanced Vegetation Index

The transformation of terrestrial vegetation condition, driven by both climate change and human activities, has been a prevalent trend in recent decades. As the planet's climate continues to shift, altering disturbance patterns and environmental factors, the vegetation dynamics are being significantly impacted globally. To describe changes in vegetation, the term "greening" and "browning" has been adopted by research communities. Greening indicates increasing leaf area index which infers vegetation restoration. The causes are reported to be various factors, including CO_2 fertilization, changes in precipitation, temperature and radiation level, land use change, and nitrogen deposition. CO_2 fertilization which refers to the elevating concentration of CO_2 in the atmosphere has been reported as a major driver[1]. In the past four decades, the greening of terrestrial vegetation has been observed by remotely sensed satellite images globally[1–6]. However, recent finding has reported that there is an indication of transition from a period of vegetation greening to a progressively widespread occurrence of remotely sensed vegetation browning[7], indicating loss in vegetation cover. The main drivers for browning include forest fire and drought, biotic factors such as insect and pathogen outbreaks, and stronger wind and storms[7] which are expected to increase in the near future due to climate change.

[1]Department of International Public Policy, Faculty of Humanities and Social Sciences, University of Tsukuba, Tsukuba, Japan. [2]Program in Economic and Public Policy (PEPP), Graduate School of Humanities and Social Sciences, University of Tsukuba, Tsukuba, Japan. [3]Environmental Engineering, Faculty of Agricultural Technology, Brawijaya University, Malang, Indonesia. [4]Information System Department, Faculty of Computer Science, Brawijaya University, Malang, Indonesia. ✉email: fatwa.ramdani.gw@u.tsukuba.ac.jp

Among these changes, vegetation covers of tropical forests stand out for their pivotal role in the Earth's carbon and energy cycles, as they store over 40% of the world's terrestrial carbon and contribute to more than 50% of global primary productivity[8]. Tropical forests in Indonesia which cover a total area of 141.7 million ha is the third largest in the world[9]. Of this, 22.1 million ha is Terrestrial National Parks (TNPs) that is categorized as protected area[10], approximately 1% of the world's protected land area[11]. A recent study by Furusawa et al.[12] reported that greening is observed in overall vegetation cover in Indonesia, with exception in areas that is highly affected by human activities. Considering the important role of Indonesian forest to global carbon sinks and greenhouse gas emission, this study observes more closely the vegetation dynamics in Indonesia's TNPs where human intervention is rather minimum.

Vegetation Indices from multispectral data are often used to describe vegetation cover/status with high temporal resolution[13–15]. For this reason, we use MODIS Enhanced Vegetation Indices (EVI) time-series imagery (MOD13Q1) to monitor the vegetation dynamics of TNPs in Indonesia from 2000 to 2022. EVI is recognized for its responsiveness in densely vegetated areas and its sensitivity to canopy variations[16], both of which are conditions commonly found in the TNP region. An increasing EVI value is indicative of a higher density or healthier vegetation cover, while decreasing EVI value indicates otherwise. In addition, we use Google Earth Engine (GEE) cloud-computing platform to enable faster and more efficient computational process.

Characteristics of vegetation in Indonesia's national parks can vary greatly from one park to another due to differences in climate, altitude, and geographic location. The types of vegetation include tropical rainforests[17–21], mangroves[22–25], savannas[26–30], and montane forests[31–35]. This study examines the greening and browning of vegetation fraction trends in 37 Indonesian TNPs in five geographical regions as listed in Table 1 [36]. To have a complete view on the vegetation dynamics, we also observe vegetation seasonality and assess anomalous years. Vegetation seasonality gives information about regularity in plant growth cycles and their timing[37]. In times of disturbances, vegetation seasonality may be affected and anomaly detection techniques[38] can be employed to identify and analyze these anomalous years. Numerous comprehensive studies have examined the influence of climate change on the heightened probability of extreme precipitation patterns[39–42], more frequent forest fires[43], and increasingly severe fire behavior[42–44]. In line with these findings, this work also investigates the interaction between precipitation dynamics and forest fire events with vegetation greening and browning trends.

Data and methods

Boundaries and land cover of the TNPs

The boundaries of Indonesia's TNPs are collected from the World Database on Protected Areas (WDPA)[36]. The land cover distribution of the observed TNPs was obtained from ESA WorldCover v200, a global land cover map in 2021 with a spatial resolution of 10 m[45]. The data consist of 11 land cover classes analyzed from Sentinel-1 and Sentinel-2 imagery, which are tree cover, shrubland, grassland, cropland, built-up area, bare/sparse vegetation, snow and ice, permanent water body, herbaceous wetland, mangroves, and moss and lichen.

Calculation of MODIS EVI value

The value range for EVI is typically between − 1 and 1. However, in healthy vegetation, EVI values usually range between 0.2 and 0.8, with higher values indicating denser and healthier vegetation. EVI value is calculated using Eq. (1),

$$EVI = \frac{2.5(NIR - Red)}{NIR + 6Red - 7.5Blue + 1)} \tag{1}$$

where NIR refers to the near-infrared band, Red refers to the red band, Blue refers to the blue band, and the coefficients 2.5, 6, 7.5, and 1 are constants that account for canopy background adjustment, aerosol resistance, and adjustments for atmospheric influences[46,47].

In this equation, NIR, Red, and Blue are atmospherically-corrected and partially atmosphere-corrected surface reflectance.

NASA LPDAAC at the USGS EROS Center provided the main data used in this study, which are Global MODIS EVI data with a 16-day temporal resolution and 250-m spatial resolution (MOD13Q1). They atmospherically corrected the EVI product, calculated it from the two-way surface reflectance, and masked it for water, clouds, heavy aerosols, and cloud shading. The GEE data catalogue offers these data as an image collection. GEE is used to process these data and the codes developed in this research are available by emailing the author upon any reasonable request. These data have been available since February 18, 2000, and are designed to reduce canopy background variations while remaining sensitive to dense vegetation conditions. Additionally, to calculate EVI, the blue band is utilized to remove residual atmospheric contamination caused by smoke and wispy clouds, as described by Huete et al.[16].

Greening and browning fraction analysis

Greening and browning analysis are conducted by assessing the EVI values' trends. We use time-series 16-day EVI images (MOD13Q1) taken from 2000 to 2022 (January-December) to produce time-series annual maximum EVI images. To investigate the significance of the time-series median maximum EVI, the Mann–Kendall trend test is used[48,49]. The null hypothesis (H_0) is that there is no trend of either a significant greening or browning ($\alpha = 0.05$) in the TNPs, and the alternative hypothesis (H_a) is that there is a trend of either a significant greening or browning ($\alpha = 0.05$) in the TNPs.

Sen's slope estimator[50] which has been widely used for similar analysis[51–53] is applied to the time-series annual maximum EVI images to separate the vegetation greening and browning fractions in the TNPs during study

No	TNP	Greening		Browning		Sen's Slope (10^{-4} yr^{-1})	R^2	Overall Status
		Fraction	Area (km^2)	Fraction	Area (km^2)			
East Indonesia		Total	17,177.68	Total	10,020.65			
1	Aketajawe Lolobata (ALA)	0.572	938.84	0.42	690.73	3.6	0.06	Greening
2	Bali Barat (BBA)	0.815	147.75[a]	0.118	21.39	30.2	0.47	Greening
3	Komodo (KA)	0.41	730.24	0.083[a]	148.46	36.1	0.44	Greening
4	Lorentz (LA)	0.579	13,645.322[b]	0.367	8,637.35	2.8	0.07	Greening
5	Manupeu Tanadaru (MTA)	0.78	391.72	0.209	104.8	16.1	0.32	Greening
6	Manusela (MA)	0.755	1,323.81	0.238	417.92	11.8	0.32	Greening
Confidence interval (95%)		0.65 ± 0.16		0.24 ± 0.14		17 ± 14		
Sulawesi		Total	4,982.61	Total	1,492.91			
7	Bantimurung Bulusaraung (BBB)	0.755	329.13	0.236	102.97[a]	12.4	0.07	Greening
8	Bogani Nani Wartabone (BWB)	0.817	2,325.8	0.176	500.77	14.9	0.41	Greening
9	Lore Lindu (LLB)	0.692	1,497.17	0.29	647.8	7.1	0.18	Greening
10	Rawa Aopa Watumohai (RWB)	0.769	830.51	0.224	241.37	20.3	0.54	Greening
Confidence interval (95%)		0.76 ± 0.08		0.23 ± 0.07		14 ± 8		
Kalimantan		Total	28,811.63	Total	8,561.70			
11	Danau Sentarum (DSC)	0.495	634.229	0.498	638.62	− 7.0	0.05	Browning
12	Tanjung Putting (TPC)	0.556	2,299.74	0.402	1,662.05	5.0	0.03	Greening
13	Bukit Baka (BBC)	0.723	1,718.58	0.27	641.23	10.7	0.18	Greening
14	Betung Kerihun (BKC)	0.854	7,010.96	0.14	1,145.28	17.7	0.64	Greening
15	Sebangau (SC)	0.813	4,852.26	0.181	1,077.40	22.1	0.53	Greening
16	Gunung Palung (GPC)	0.791	859.2	0.202	219.64[a]	16.0	0.29	Greening
17	Kayan Mentarang (KMC)	0.765	9,770.26	0.229	2,920.7[b]	15.0	0.39	Greening
18	Kutai (KC)	0.861	1,666.40	0.133	256.78	31.2	0.46	Greening
Confidence interval (95%)		0.73 ± 0.09		0.26 ± 0.08		14 ± 9		
Jawa		Total	3,123.85	Total	773.45			
19	Alas Purwo (APD)	0.794	351.22	0.191	85.58	18.4	0.38	Greening
20	Bromo Tengger Semeru (BTD)	0.911	462.09	0.083	42.09	39.5	0.57	Greening
21	Meru Betiri (MBD)	0.716	469.86	0.129	84.67	22.4	0.5	Greening
22	Gunung Ciremai (GCD)	0.669	99.65	0.324	48.24	12.8	0.23	Greening
23	Gunung Gede (GGD)	0.832	203.51	0.161	39.31	20.3	0.31	Greening
24	Gunung Halimun (GHD)	0.789	694.97	0.203	179.001	17.4	0.24	Greening
25	Gunung Merbabu (GMD)	0.729	42.66	0.26	15.21	9.8	0.14	Greening
26	Ujung Kulon (UKD)	0.499[a]	554.23	0.206	228.83	15.4	0.28	Greening
27	Baluran (BD)	0.823	245.66	0.169	50.52	23.9	0.29	Greening
Confidence interval (95%)		0.75 ± 0.63		0.19 ± 0.13		14 ± 18		
Sumatra		Total	25,875.58	Total	8,177.35	0		
28	Berbak (BE)	0.734	1,042.04	0.259	367.04	18.9	0.51	Greening
29	Batang Gadis (BGE)	0.828	604.81	0.165	120.50	16.3	0.33	Greening
30	Bukit Barisan Selatan (BBE)	0.802	2,543.45	0.19	602.3	16.2	0.36	Greening
31	Bukit Dua Belas (BDE)	0.757	416.03	0.236	129.63	13.7	0.28	Greening
32	Bukit Tiga Puluh (BTE)	0.592	858.03	0.401	580.31	5.7	0.09	Greening
33	Gunung Leuser (GLE)	0.664	5,534.02	0.328	2,735.86	7.9	0.12	Greening
34	Sembilang (SBE)	0.637	1,713.42	0.258	694.32	18.3	0.46	Greening
35	Siberut (SE)	0.828	1,477.21	0.165	293.36	21.6	0.47	Greening

Continued

No	TNP	Greening		Browning		Sen's Slope (10^{-4} yr^{-1})	R^2	Overall Status
		Fraction	Area (km^2)	Fraction	Area (km^2)			
36	Kerinci Seblat (KSE)	0.829	11,291.7	0.164	2,235.10	16.7	0.51	Greening
37	Tesso Nilo (TNE)	0.481	394.87	0.511	418.93	1.5	0.005	Greening
Confidence interval (95%)		0.66 ± 0.08		0.25 ± 0.08		13 ± 4		

Table 1. Greening and Browning Fraction Trends of Terrestrial National Parks in Indonesia from 2000 to 2022.

period. The linear regression slope is generated to provide additional information on the vegetation greening or browning fraction change rates.

To map water seasonality, we utilized data from the Joint Research Centre (JRC) Global Surface Water Mapping Layers, v1.4. This dataset includes maps detailing the location and temporal distribution of surface water from 1984 to 2021, along with statistics on the extent and changes of these water surfaces. Water seasonality is measured in months, with a minimum value of 0 and a maximum value of 12, representing the number of months water is present. The data are available in the GEE data catalogue.

Analysis of anomalous year

Anomalous year refer to the years where greenness level in the observed TNPs is deviated from the median value. The anomalous years are detected by comparing the time-series annual mean EVI, presented in Day-of-Year calendar system (DOY), with the long-term median EVI (2000–2022) using the Mann−Whitney U test[54]. The magnitudes of the anomalies identified for the anomalous years are visualized spatially using the Z-score statistical measure.

The formula to calculate the EVI Z-score is presented in Eq. (2),

$$Z_n = \frac{(X_n - \mu)}{\sigma} \tag{2}$$

where Z_n is the Z-score of EVI of the n year, X_n is the EVI of n year to calculate the Z-score of the n year, μ is the mean of EVI during the study period, and σ is the standard deviation of EVI during the study period.

Validation

We validate our findings by qualitatively comparing the results with various data sources, i.e., Google Earth images, government websites, and previous studies. Additionally, we gather reports published by the TNP offices and related government agencies, as well as relevant previous studies and news from online platforms to understand any notable phenomena occurring in the TNPs that may link to our results.

Results and discussion

Greening and browning

Result of the greening and browning analysis is presented in Table 1. Every location exhibited varying fractions and areas of both greening and browning. Then there is Sen's slope[50] value for each TNP, which is an estimator that has been widely used in vegetation and forest mapping research to identify the greening or browning status of interannual time series[51–53]. A positive Sen's slope value is observed in areas where the fraction and area of greening surpasses that of browning, and the overall status of the TNP is greening. Conversely, when the reverse situation unfolds, the overall status of the TNP is browning.

Of the 37 TNPs observed in this study, 36 TNPs experienced overall greening. One TNP which experienced overall browning is Danau Sentarum in Kalimantan region. This result is aligned with the global vegetation trends[1,55,56].

As visual representation of the overall greening location, Fig. 1 shows the trends in Bromo-Tengger-Semeru TNP which has the highest greening fraction compared to other TNPs. Bromo-Tengger-Semeru TNP is predominantly covered by trees and grassland (Fig. 1a), so that the greening and browning trend of this location is mainly linked the two land cover types. Forest and land fires during the dry season cause temporary browning[57], but the upcoming rainy seasons provides favorable conditions for the vegetation to rejuvenate and lead to greening. While the relation of land cover types and greening browning trends are complex[58], in this area tree cover exhibits a significant greening trend indicated by increasing Sen's slope, while areas that exhibits browning is mostly in grasslands which tend to suffer the most severe consequences of forest fires[59,60] (Fig. 1b).

Figure 2 shows visual representation of the trends in Danau Sentarum TNP where overall status of browning occurred. The main land cover is tree cover and permanent water bodies, with some areas of grassland and shrubland (Fig. 2a). Browning is identified in fairly all of the areas, particularly in the surrounding of water bodies (Fig. 2b). This national park is a natural dam and a distinctive freshwater fish habitat formed within a flat basin or floodplain that experiences varying water levels throughout the year due to rainfall and the inflow of water from the Kapuas River system[61], a major river in Kalimantan Island. Seasonality variation of water bodies in the Danau Sentarum National Park is also revealed in Fig. 2c where some parts are covered with water bodies at all months in a year, such areas are presented in dark blue color. Meanwhile, other parts are only covered with water for several months in a year. The light blue areas shows that water bodies only present during the rainy season and then recede significantly in the dry season. Land degradation due to illegal logging and land clearing

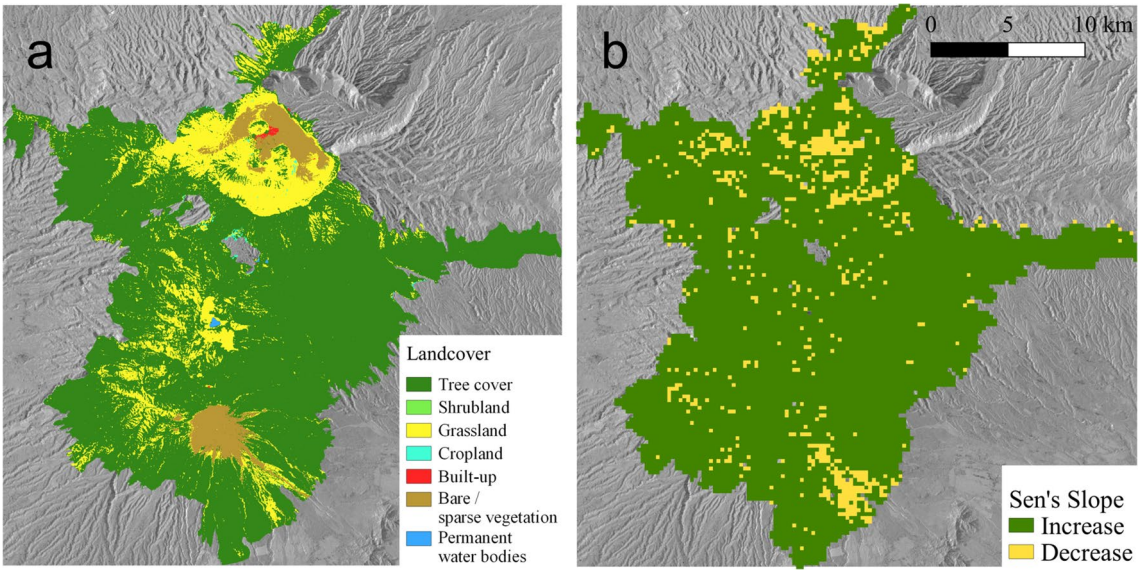

Figure 1. Bromo Tengger Semeru TNP: (**a**) land cover; (**b**) Sen's slope-based increase (greening) and decrease (browning) trends. This figure was created using QGIS Desktop version 3.28.3-Firenze, available at https://download.qgis.org/downloads/

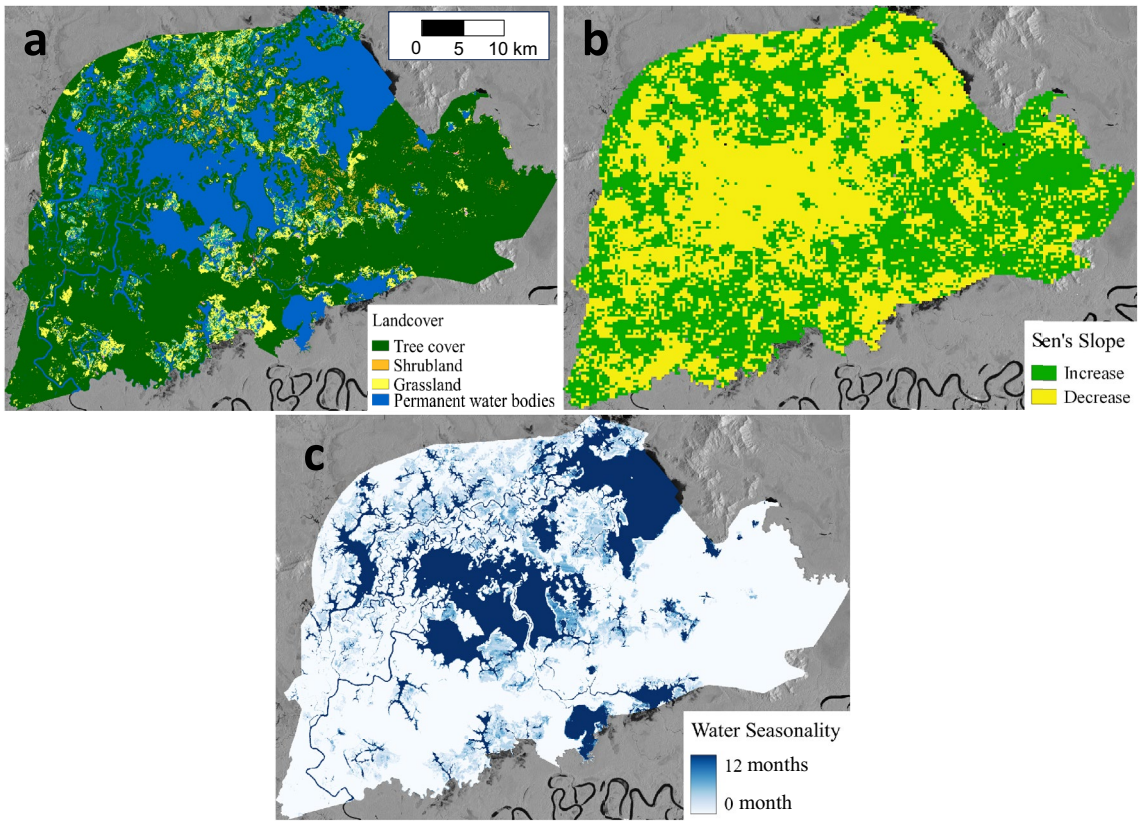

Figure 2. Danau Sentarum TNP: (**a**) land cover; (**b**) Sen's slope-based increase (greening) and decrease (browning) trends; and (**c**) water seasonality. This figure was created using QGIS Desktop version 3.28.3-Firenze, available at https://download.qgis.org/downloads/

around and within the national park area, as well as direct overexploitation of resources has been reported in this location[62]. Within year 2000 to 2013, about 6% of the total area was converted to oil palm plantation[63], inducing ecosystem alteration. The same study also reported that major decrease in area was observed for forest and shrubland (bush), while dry agriculture, grassland and barren area were increased. High frequency of fire was

also observed in Danau Sentarum, with the causes linked to fire usage as tool for land clearing, weapon in land disputes, accidental fire from illegal logging and fire connected with resource extraction[64,65].

Vegetation seasonality and anomalous year detection

The TNPs in Indonesia experience seasonal vegetation dynamics resulting from the varying responses of vegetation from rainy to dry season changes. Table 2 shows seasonality (peaks and troughs) and anomalous years in the Terrestrial National Parks of Indonesia (2000–2022). Figure 3 shows the comparison between precipitation rate from Climate Hazards Group InfraRed Precipitation with Station (CHIRPS) dataset with vegetation phenology

No	TNPs	Seasonality (DOY Mode ± Stdev)		P–T (days)	T–P (days)	Anomalous years
		Peaks (P)	Troughs (T)			
Indonesia Timur						
1	Aketajawe Lolobata (ALA)	65 ± 73.7	193 ± 135.2	128	237	2006*; 17*
2	Bali Barat (BBA)	65 ± 29.5	321 ± 55.5	256	109	2016*; 22*; 10**
3	Komodo (KA)	33 ± 21.4	321 ± 34.5	288	77	–
4	Lorentz (LA)	49 ± 51.4	209 ± 150.0	160	205	2010*
5	Manupeu Tanadaru (MTA)	49 ± 27.8	353 ± 50.7	304	61	2012*; 13*; 09**; 11**; 10***; 16***
6	Manusela (MA)	65 ± 45.1	177 ± 146.3	112	253	2015*; 17**
Sulawesi						
7	Bantimurung Bulusaraung (BBB)	49 ± 50.3	1 ± 42.5	317	48	2016**
8	Bogani Nani Wartabone (BWB)	65 ± 76.7	209 ± 129.9	144	221	2008*
9	Lore Lindu (LLB)	273 ± 81.2	353 ± 59.7	80	285	2022*
10	Rawa Aopa Watumohai (RWB)	49 ± 47.9	161 ± 130.9	112	253	2000*; 04*; 16**
Kalimantan						
11	Danau Sentarum (DSC)	257 ± 109.5	1 ± 50.4	109	256	2010*; 14*
12	Tanjung Putting (TPC)	49 ± 65.2	289 ± 61.7	240	125	2007*; 08*; 11*; 13*; 14*; 05**; 16***
13	Bukit Baka (BBC)	65 ± 80.7	33 ± 72.3	333	32	2002*; 05*; 13**
14	Betung Kerihun (BKC)	273 ± 84.4	33 ± 54.5	125	240	–
15	Sebangau (SC)	65 ± 77.4	17 ± 47.1	317	48	2000*; 13*; 19**
16	Gunung Palung (GPC)	65 ± 75.5	1 ± 46.9	301	64	2000*
17	Kayan Mentarang (KMC)	257 ± 91.0	17 ± 55.4	125	240	–
18	Kutai (KC)	65 ± 78.6	289 ± 73.8	224	141	–
Jawa						
19	Alas Purwo (APD)	33 ± 30.8	321 ± 87.1	288	77	2010*; 20*; 16**
20	Bromo Tengger Semeru (BTD)	17 ± 62.6	305 ± 34.2	288	77	2003*; 04*; 13*; 15*; 17*; 06**; 09**; 14**; 20**
21	Meru Betiri (MBD)	33 ± 41.1	305 ± 67.6	272	93	2010*; 16*
22	Gunung Ciremai (GCD)	33 ± 73.1	337 ± 44.8	304	61	–
23	Gunung Gede (GGD)	273 ± 83.9	289 ± 44.2	16	349	2016*
24	Gunung Halimun (GHD)	65 ± 54.6	353 ± 30.5	288	77	–
25	Gunung Merbabu (GMD)	145 ± 57.7	337 ± 51.6	192	173	–
26	Ujung Kulon (UKD)	65 ± 39.3	353 ± 41.6	288	77	–
27	Baluran (BD)	33 ± 24.1	321 ± 57.5	288	77	2010*; 13*; 22*
Sumatra						
28	Berbak (BE)	273 ± 93.9	337 ± 37.5	64	301	–
29	Batang Gadis (BGE)	65 ± 86.4	305 ± 45.6	240	125	2011*
30	Bukit Barisan Selatan (BBE)	33 ± 54.5	289 ± 28.8	256	109	2000*; 21**
31	Bukit Dua Belas (BDE)	97 ± 81.3	17 ± 55.1	285	80	2016*
32	Bukit Tiga Puluh (BTE)	321 ± 78.8	1 ± 63.7	45	320	–
33	Gunung Leuser (GLE)	257 ± 92.5	289 ± 32.6	32	333	2000*
34	Sembilang (SBE)	65 ± 73.4	353 ± 36.7	288	77	–
35	Siberut (SE)	257 ± 86.6	321 ± 53	64	301	2021*; 22*
36	Kerinci Seblat (KSE)	65 ± 44.6	1 ± 39.1	301	64	2011*
37	Tesso Nilo (TNE)	97 ± 88.9	17 ± 68.6	285	80	2020*; 14**

Table 2. Seasonality (peaks and troughs) and anomalous years in the Terrestrial National Parks of Indonesia (2000–2022). *$\alpha < 0.05$; ** $\alpha < 0.01$; *** $\alpha < 0.001$.

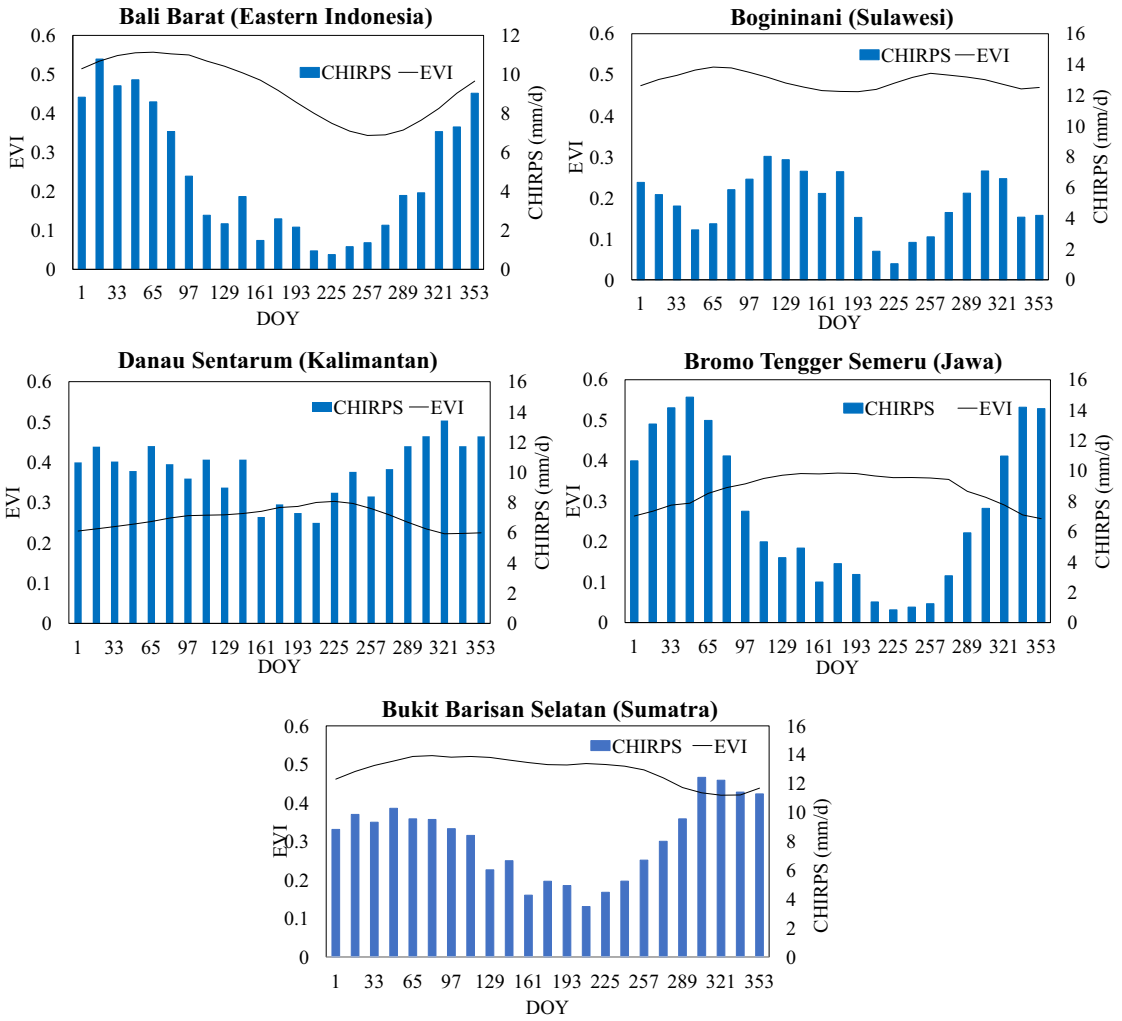

Figure 3. Seasonal vegetation phenology variation examples in several TNPs in the five regions derived from the long-term (2000–2022) median EVI data compared to precipitation of CHIRPS data.

represented by EVI value in several TNPs in the five regions. It shows that most parks exhibit peak greenness at the end of the rainy season, when precipitation is high and vegetation response is at its strongest. Conversely, these parks experience troughs in greenness during the dry season, when precipitation decreases and vegetation response is reduced. The TNPs in each region show 5–8-month greening periods from the peaks to the troughs and 4–7-month periods from the troughs to the peaks. The TNPs may exhibit two peaks of precipitation rate seasons (i.e., Bogininani—LLD, Sulawesi and Bukit Barisan Selatan—BBE, Sumatra) due to the varying responses of vegetation to local physical and climatic factors (i.e., the aspect, solar radiation, and temperature).

An IPCC special report on climate change and land reveals that climate change in tropical regions will cause both greening and browning[66]. When global warming results in reduced rainfall, it diminishes biomass production, leading to localized warming[67–69]. Conversely, in areas where warming causes increased rainfall, it fosters greening. Browning of the land reduces evapotranspiration and atmospheric humidity. The warming caused by decreased evapotranspiration is amplified by reduced cloud cover, resulting in increased solar radiation, while the warming is tempered by a decline in water vapor greenhouse radiation.

Moreover, according to research conducted by Franklin et al.[70], the impact of global warming on the water balance could potentially wield a more substantial influence compared to the direct effects of temperature on vegetation. This highlights the importance of managing water resources and maintaining healthy ecosystems to ensure the continued success of conservation and restoration efforts.

The TNPs in all regions of Indonesia experienced anomalous years during the study period, as presented in Table 2. Anomalous years are assessed by comparing the annual time series and long-term median EVI value of each location. These anomalies could be attributed to various factors such as extreme climate events[71], human activities and climate change[72], or other environmental disturbances. Regionally, the TNPs in Eastern Indonesia experienced more anomalous years than the TNPs in other regions. In contrast, the TNPs in Sumatra rarely experienced anomalous years. Some studies have shown that precipitation dynamics in Indonesia is also affected by El Niño Southern Oscillation (ENSO) events[73–76], particularly in eastern part of the country where significantly linear correlation between ENSO events and precipitation response was observed[77].

Compared to other locations, Bromo-Tengger-Semeru TNP experienced highest frequency of anomalous year. The anomaly trend shifted from low EVI values in 2003, 2004, and 2006 to moderate and high EVI values in 2009, 2013, 2014, 2015, 2017, and 2020 (Fig. 4).

Validation

In Fig. 5, we can observe greening and browning fraction phenomena by contrasting images from two periods of 2000 – 2010s and 2020s in various locations across Bromo Tengger Semeru National Park. This TNP is located within highly active volcanic areas. In this locale, browning is identified in BTD 2 and BTD 4 areas where the occurrence can be attributed also lava and pyroclastic flow from recurring eruptions[78,79], and also to the hotspot area from forest fire events in the past 20 years[80,81]. The frequent flow of molten materials renders the ground unsuitable for vegetation growth, consequently leading to the occurrence of browning events. In the case of greening, there is an intriguing connection between wildfires and greening in the area. When an area undergoes

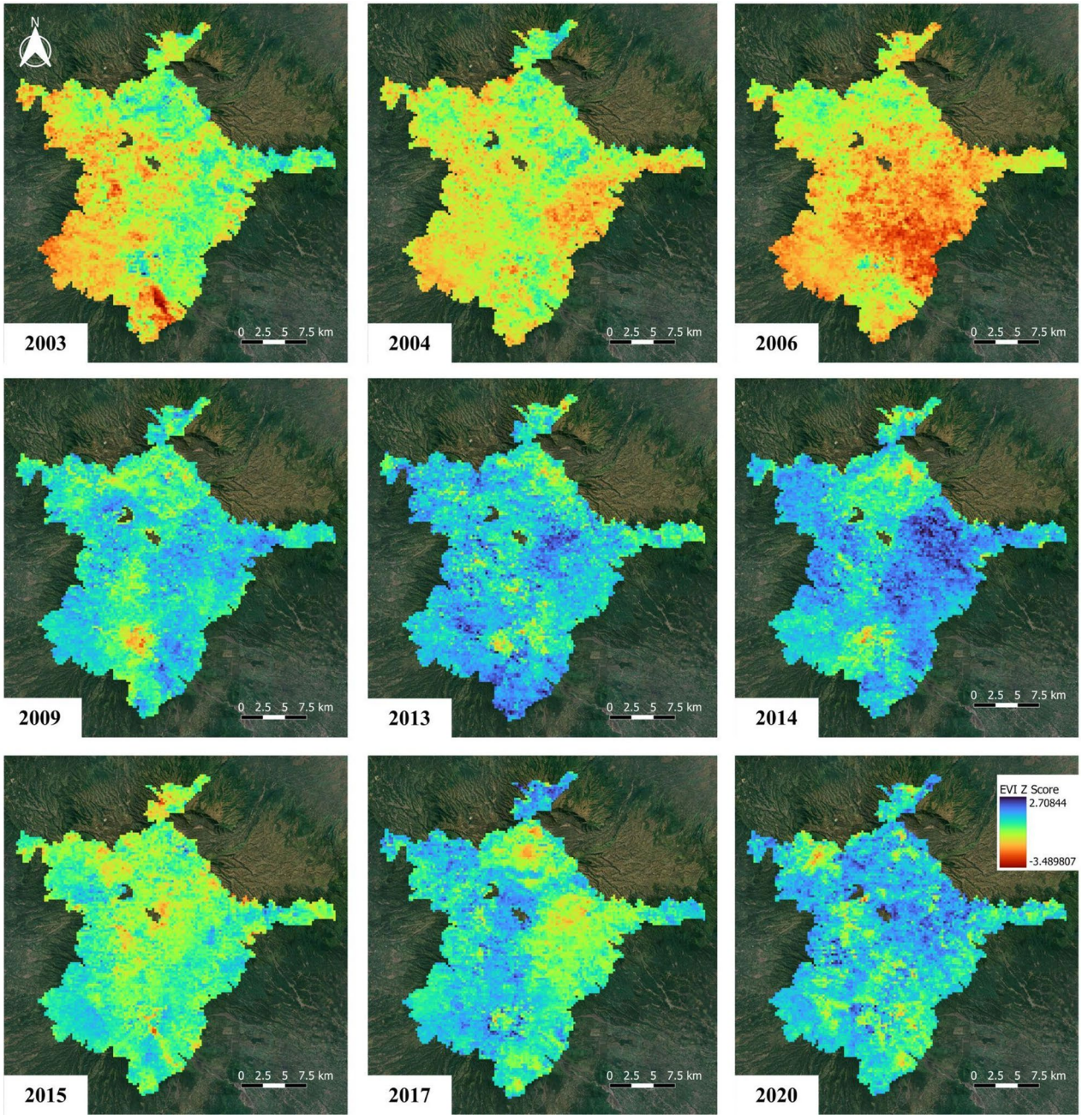

Figure 4. The Bromo Tengger Semeru National Park experienced anomalous years spanning from 2003 to 2020. Between 2003 and 2006, this renowned national park encountered notably low EVI values, while from 2009 to 2020, it experienced a shift towards moderate and high EVI values. Background: Optical imagery data of Google Map. This figure was created using QGIS Desktop version 3.28.3-Firenze, available at https://download.qgis.org/downloads/

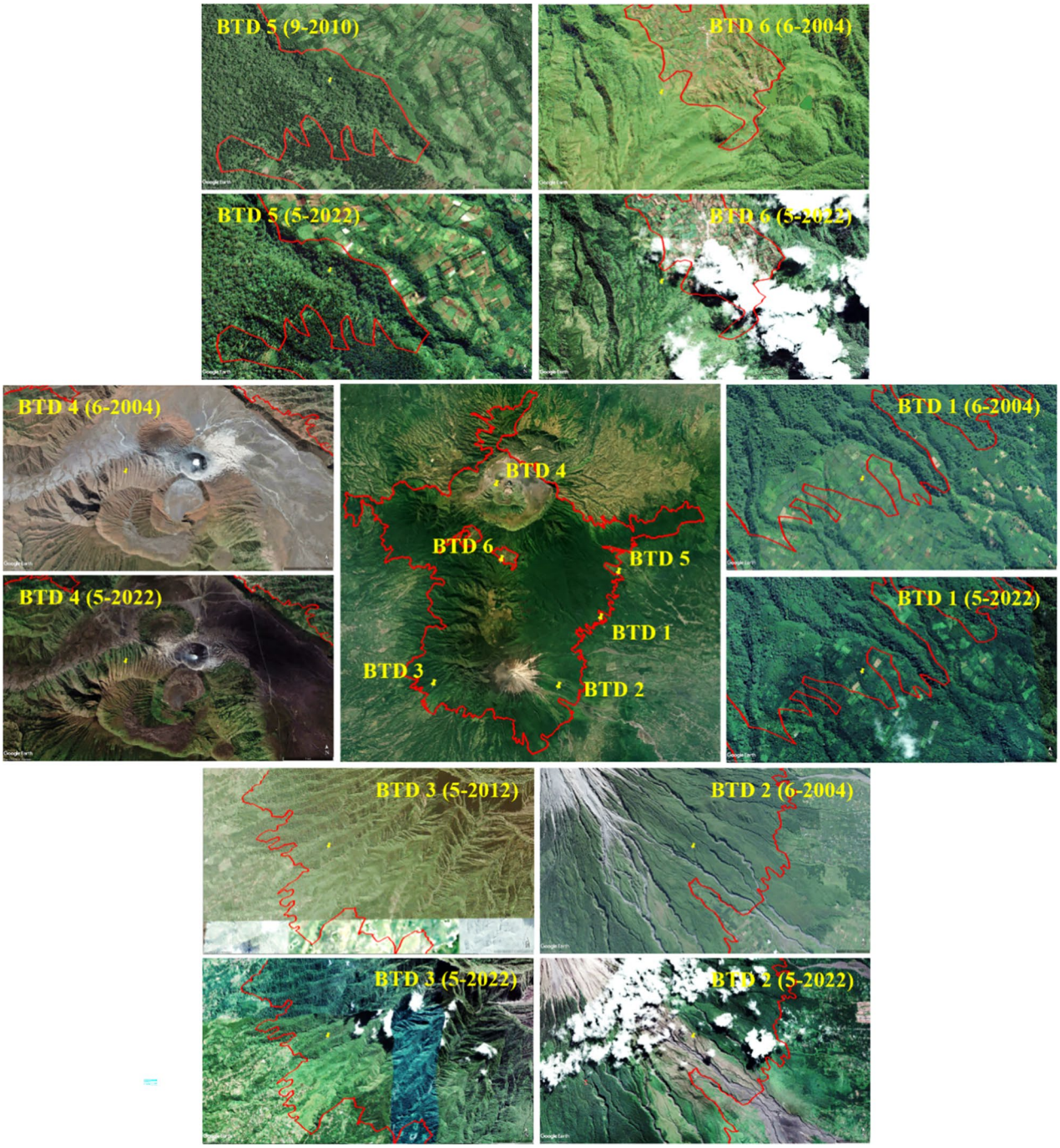

Figure 5. Greening and Browning in the Bromo Tengger Semeru (BTD) National Park. Greening areas: BTD1 (113.011°, – 8.083°), BTD3 (112.845°, – 8.113°), BTD4 (112.938°, 7.944°), BTD5 (113.036°, – 8.045°), and BTD6 (112.93°, – 8.012°); Browning areas: BTD2 (112.959°, – 8.137°). This figure was created using QGIS Desktop version 3.28.3-Firenze, available at https://download.qgis.org/downloads/

greening, it also heightens the likelihood of wildfires, particularly in regions abundant with tall grasses. The presence of these tall grasses results in an escalation of fuel loads, thereby facilitating the rapid spread of intense wildfires.

Figure 6 shows the location of wildfires that transpired between 2000 and 2022. By comparing this with Fig. 5, we observe recurring incidents of wildfires in BTD 4 and BTD 6 regions, while a larger-scale wildfire event affected BTD 3 in both 2016 and 2019. Interestingly, most of the areas impacted by wildfires within BTD demonstrate signs of greening. Nevertheless, it is essential to note that greening is not solely attributed to wildfire occurrences, as similar vegetative improvements are observed in other regions where fires did not take place.

During the warm phase events of the El Niño–Southern Oscillation (ENSO), Indonesia experiences deficient rainfall. This results in drier conditions that can stress rainforests and affect their health, and these drier

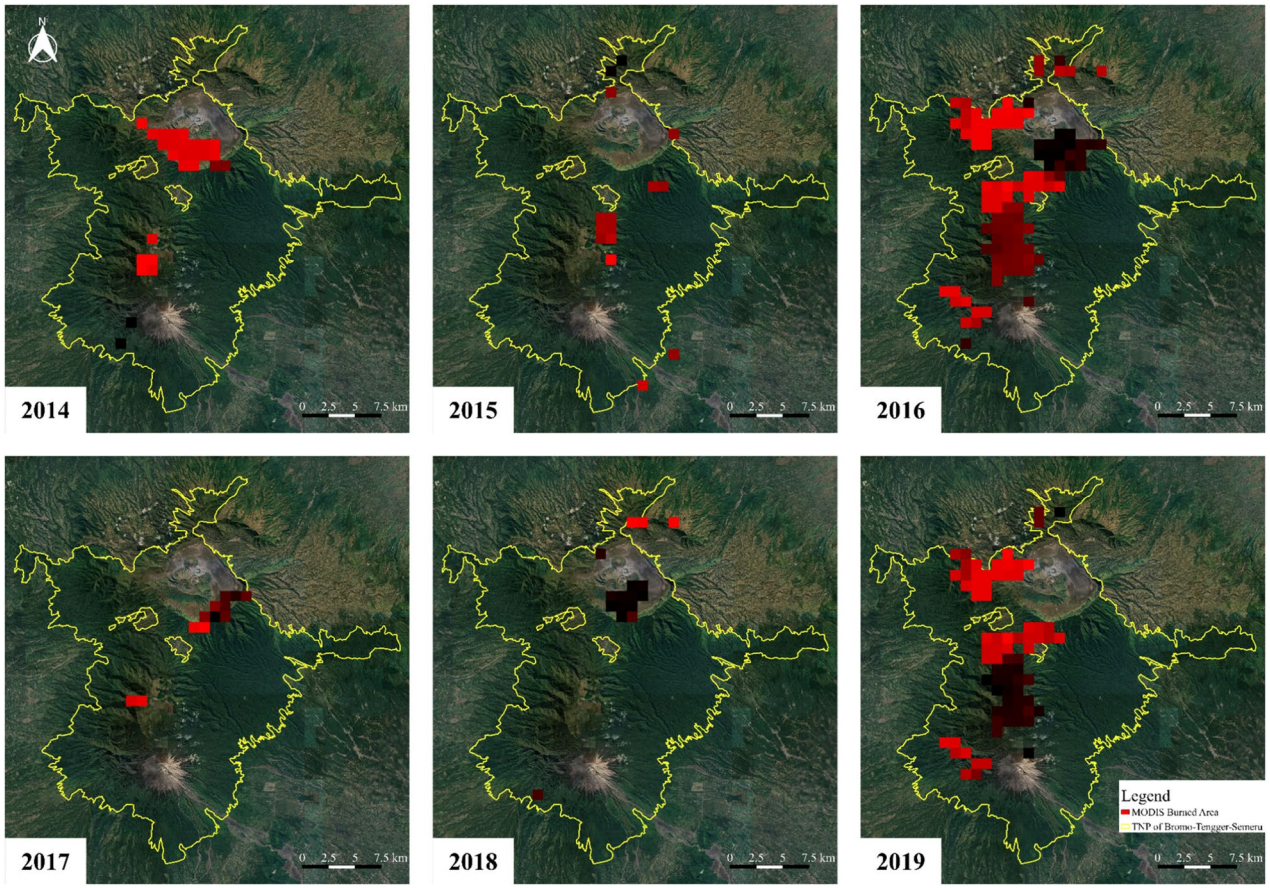

Figure 6. Burned area in the Bromo Tengger Semeru (BTD) National Park from 2014 to 2019 using data of MODIS MCD64A1. The MCD64A1 burned-area mapping approach employs 500m MODIS Surface Reflectance imagery coupled with 1km MODIS active fire observations. This figure was created using QGIS Desktop version 3.28.3-Firenze, available at https://download.qgis.org/downloads/

conditions can also lead to wildfires. The anomaly pattern of the extreme El Niño events in 2016 and 2019 caused large burned areas in BTD National Park.

Conversely, during La Niña events (the cool phase of ENSO), Indonesia tends to receive excess rainfall. This can lead to flooding and soil erosion, impacting rainforest ecosystems. However, it can also result in a few wildfire events, as seen with the small burned area in 2018, as shown in Fig. 6.

Recommendations for TNP management

Seasonality anomalies were observed across all regions, stemming from both natural and anthropogenic factors, with climate change as a significant contributor. Mitigating the escalating atmospheric carbon dioxide concentration, a key driver of adverse climate change effects, is particularly facilitated by fostering increased vegetation or greening. Within this study, areas exhibiting browning are identified as those predominantly covered by grassland, undergoing forest-to-other-land-cover conversion with diminished vegetation index, and experiencing disturbances from human activities in their surrounding environments. Despite the inevitable impact of climate change on seasonality anomalies influencing vegetation dynamics in terrestrial national parks, this study explores measures to enhance their resilience. Implementation of active reforestation to the degraded land and application Assisted Natural Regeneration which involves management intervention to facilitate forest regeneration has shown improvement in forest conditions in various areas[82–85]. A study by Bruner et al.[86] also explained that fundamental managerial tasks, such as the enforcement of regulations and the establishment of distinct boundaries, have proven effective in enhancing the management efficiency of protected areas including TNPs. Additionally, forest fire management and prevention of uncontrolled wildfire is also a significant factor in preserving the balance of vegetation dynamics.

Conclusions

The study has successfully monitored the spatiotemporal vegetation dynamics of TNPs in Indonesia using MOD13Q1 EVI data from 2000 to 2022, supported by GEE cloud computing power. The findings indicate that most TNPs, except for Danau Sentarum, have experienced varying degrees of greening, with Kalimantan dominating the largest area of greening fraction, followed by Sumatera and Eastern Indonesia. On the other hand, Eastern Indonesia has a large area of browning fraction, followed by Sumatera and Kalimantan. The Java region

has a relatively small area coverage, but the highest portion of the greening fraction is found in Bromo-Tengger-Semeru National Park, which may be affected by land fires and forest encroachment for economic activities.

The study also reveals that most TNPs in Indonesia exhibit anomalous years during the 2000–2022 period, and the peaks and troughs of vegetation dynamics occur several weeks after the rainy and dry seasons, indicating varying responses to local physical and climatic factors.

These findings have important implications for the sustainable management of TNPs in Indonesia, and future studies should investigate the driving factors influencing vegetation dynamics of TNPs and their impacts at the national and global scales.

Data availability

The raw datasets used and/or analysed during the current study are available at Earth Engine Data Catalogue, and the processed data are available by contacting the corresponding author upon reasonable request.

Received: 5 December 2023; Accepted: 2 August 2024
Published online: 06 August 2024

References

1. Zhu, Z. *et al.* Greening of the Earth and its drivers. *Nat. Clim. Change* **6** (2016).
2. Macias-Fauria, M., Forbes, B. C., Zetterberg, P. & Kumpula, T. Eurasian Arctic greening reveals teleconnections and the potential for structurally novel ecosystems. *Nat. Clim. Change* **2** (2012).
3. Piao, S. *et al.* Detection and attribution of vegetation greening trend in China over the last 30 years. *Glob. Change Biol.* **21** (2015).
4. Chen, C. *et al.* China and India lead in greening of the world through land-use management. *Nat. Sustain.* **2** (2019).
5. Myers-Smith, I. H. *et al.* Complexity revealed in the greening of the Arctic. *Nat. Clim. Change.* https://doi.org/10.1038/s41558-019-0688-1 (2020).
6. Li, W. *et al.* Complex causes and consequences of rangeland greening in South America—Multiple interacting natural and anthropogenic drivers and simultaneous ecosystem degradation and recovery trends. *Geogr. Sustain.* **1**, 304–316 (2020).
7. Liu, Q. *et al.* Vegetation browning: Global drivers, impacts, and feedbacks. *Trends Plant Sci.* https://doi.org/10.1016/j.tplants.2023.03.024 (2023).
8. Dias, T. C., Silveira, L. F., Pironkova, Z. I. & Francisco, M. R. Greening and browning trends in a tropical forest hotspot: Accounting for fragment size and vegetation indices. *Remote Sens. Appl.* **26** (2022).
9. Butler, R. A. A Place out of time: Tropical rainforests and the Perils they face—Information on tropical forests, deforestation, and biodiversity. https://rainforests.mongabay.com/ (2020).
10. MOEF. The State of Indonesia's Forests 2022. https://phl.menlhk.go.id/publikasi/the-state-of-indonesias-forests-2022-towards-folu-net-sink-2030/ (2020).
11. WDPA. Discover the world's protected and conserved areas. *Prot. Planet* (2023).
12. Furusawa, T. *et al.* Time-series analysis of satellite imagery for detecting vegetation cover changes in Indonesia. *Sci. Rep.* **13** (2023).
13. Sarvia, F., Petris, S. De & Borgogno-Mondino, E. Exploring climate change effects on vegetation phenology by MOD13Q1 Data: The piemonte region case study in the period 2001–2019. https://doi.org/10.3390/agronomy11030555 (2021).
14. Jönsson, P. & Eklundh, L. Seasonality extraction by function fitting to time-series of satellite sensor data. *IEEE Trans. Geosci. Remote Sens.* **40** (2002).
15. Beeri, O. & Peled, A. Spectral indices for precise agriculture monitoring. *Int. J. Remote Sens.* **27** (2006).
16. Huete, A. *et al.* Overview of the radiometric and biophysical performance of the MODIS vegetation indices. *Remote Sens. Environ.* **83**, 195–213 (2002).
17. Dwiyahreni, A. A. *et al.* Forest cover changes in indonesia's terrestrial national parks between 2012 and 2017. *Biodiversitas* **22**, 1235–1242 (2021).
18. Sutomo & van Etten, E. J. B. Fire impacts and dynamics of seasonally dry tropical forest of East Java, Indonesia. *Forests* **14** (2023).
19. Firdaus, R., Nakagoshi, N. & Idris, A. Sustainability assessment of humid tropical watershed: A case of Batang Merao Watershed, Indonesia. *Proc. Environ. Sci.* **20** (2014).
20. Aparajita Datta and Lucy Kemp. Hornbill natural history and conservation. *Hornbill Natl. Hist. Conserv.* **3** (2022).
21. Wibowo, R. H. *et al.* Analysis of soil bacterial diversity from tropical rainforest and oil palm plantation in Jambi, Indonesia by 16S rRNA-DGGE Profiles. *J. Trop. Biodivers. Biotechnol.* **7** (2022).
22. Asadi, M. A. & Pambudi, G. S. Diversity and biomass of mangrove forest within Baluran National park, Indonesia. *AACL Bioflux* **13** (2020).
23. Poedjirahajoe, E., Sulityorini, I. S. & Komara, L. L. Short communication: Species diversity of mangrove in kutai national park, East Kalimantan, Indonesia. *Biodiversitas* **20** (2019).
24. Prihantono, J., Nakamura, T., Nadaoka, K., Wirasatriya, A. & Adi, N. S. Rainfall variability and tidal inundation influences on mangrove greenness in Karimunjawa National Park, Indonesia. *Sustainability (Switzerland)* **14** (2022).
25. Purwanto, A. D., Wikantika, K., Deliar, A. & Darmawan, S. Decision tree and random forest classification algorithms for mangrove forest mapping in Sembilang National Park, Indonesia. *Remote Sens (Basel)* https://doi.org/10.3390/rs15010016 (2023).
26. Sutomo & van Etten, E. Savanna plant communities in the wetter parts of the Indonesian archipelago. *Folia Geobot* **56** (2021).
27. Sutomo & van Etten, E. Spatial and temporal patterns of fires in tropical savannas of Indonesia. *Singap. J. Trop. Geogr.* **39** (2018).
28. Potter, A. B., Imron, M. A., Pudyatmoko, S. & Hutchinson, M. C. Short-term plant-community responses to large mammalian herbivore exclusion in a rewilded Javan savanna. *PLoS ONE* **16** (2021).
29. Karraker, N. E., Dikari Kusrini, M., Atutubo, J. R., Healey, R. M. & Yusratul, A. Non-marine turtle plays important functional roles in Indonesian ecosystems. *Ecol. Evol.* **10** (2020).
30. Sutomo. Vegetation Composition of Savanna Ecosystem as a Habitat for the Komodo Dragon (Varanus komodoensis) on Padar and Komodo Islands, Flores East Nusa Tenggara Indonesia. *J. Trop. Biodivers. Biotechnol.* **5** (2020).
31. Rozak, A. H. & Setiadi, T. Modeling of tree growth after forest fire in Mount Ciremai National Park, Indonesia. *Biotropia (Bogor)* **23** (2016).
32. Devenish, C. *et al.* Biological richness of Gunung Slamet, Central Java, and the need for its protection. *ORYX* **56** (2022).
33. Rahajoe, J. S. *et al.* Decomposition rate of some dominant tree species in Low montane forest of Gunung Halimun Salak National Park, West Java-Indonesia. in *IOP Conference Series: Earth and Environmental Science* vol. 762 (2021).
34. Culmsee, H., Pitopang, R., Mangopo, H. & Sabir, S. Tree diversity and phytogeographical patterns of tropical high mountain rain forests in Central Sulawesi, Indonesia. *Biodivers. Conserv.* **20** (2011).
35. Marshall, A. J. Are montane forests demographic sinks for bornean white-bearded gibbons hylobates albibarbis? *Biotropica* **41** (2009).

36. UNEP-WCMC and IUCN. Protected Planet: The World Database on Protected Areas (WDPA) and World Database on Other Effective Area-based Conservation Measures (WD-OECM) [Online], November 2022, Cambridge, UK: UNEP-WCMC and IUCN. *Cambridge, UK: UNEP-WCMC and IUCN* (2022).
37. Sianturi, R., Jetten, V. G. & Sartohadi, J. Mapping cropping patterns in irrigated rice fields in West Java: Towards mapping vulnerability to flooding using time-series MODIS imageries. *Int. J. Appl. Earth Observ. Geoinf.* **66** (2018).
38. Meroni, M., Fasbender, D., Rembold, F., Atzberger, C. & Klisch, A. Near real-time vegetation anomaly detection with MODIS NDVI: Timeliness vs accuracy and effect of anomaly computation options. *Remote Sens. Environ.* **221** (2019).
39. O'Gorman, P. A. Sensitivity of tropical precipitation extremes to climate change. *Nat. Geosci.* **5** (2012).
40. O'Gorman, P. A. Precipitation extremes under climate change. *Current Climate Change Reports* vol. 1 Preprint at https://doi.org/10.1007/s40641-015-0009-3 (2015).
41. Ge, F. *et al.* Risks of precipitation extremes over Southeast Asia: Does 1.5 °c or 2 °c global warming make a difference? *Environ. Res. Lett.* **14** (2019).
42. Bläckberg, C. P. O. & Singh, M. S. Increased large-scale convective aggregation in CMIP5 projections: Implications for tropical precipitation extremes. *Geophys. Res. Lett.* **49** (2022).
43. Mansoor, S. *et al.* Elevation in wildfire frequencies with respect to the climate change. *J. Environ. Manag.* https://doi.org/10.1016/j.jenvman.2021.113769 (2022).
44. Flannigan, M. D., Stocks, B. J. & Wotton, B. M. Climate change and forest fires. *Sci. Total Environ.* **262** (2000).
45. Zanaga, D., Kerchove RvD., Daems, D., Keersmaecker, WD., Brockmann, C., Kirches, G., Wevers, J., Cartus, O., Santoro, M. & Fritz, S. ESA WorldCover 10 m 2021 V200. 10.5281/zenodo.7254221 (2022).
46. Huete, A. A comparison of vegetation indices over a global set of TM images for EOS-MODIS. *Remote Sens. Environ.* **59**, 440–451 (1997).
47. Huete, A., Justice, C. & Liu, H. Development of vegetation and soil indices for MODIS-EOS. *Remote Sens. Environ.* **49**, 224–234 (1994).
48. Kendall, M. G. *Rank Correlation Methods* 4th edn. (Charles Griffin, 1975).
49. Mann, H. B. Nonparametric tests against trend. *Econometrica* **13**, 245 (1945).
50. Sen, P. K. Estimates of the regression coefficient based on Kendall's Tau. *J. Am. Stat. Assoc.* **63**, 1379–1389 (1968).
51. Sun, W., Song, H., Yao, X., Ishidaira, H. & Xu, Z. Changes in remotely sensed vegetation growth trend in the Heihe Basin of Arid Northwestern China. *PLoS ONE* **10**, e0135376 (2015).
52. Reygadas, Jensen & Moisen. Forest degradation assessment based on trend analysis of MODIS-Leaf Area Index: A case study in Mexico. *Remote Sens (Basel)* **11**, 2503 (2019).
53. Liu, Y. *et al.* Correlations between urbanization and vegetation degradation across the world's metropolises using DMSP/OLS nighttime light data. *Remote Sens. (Basel)* **7**, 2067–2088 (2015).
54. Mann, H. B. & Whitney, D. R. On a test of whether one of two random variables is stochastically larger than the other. *Ann. Math. Stat.* **18**, 50–60 (1947).
55. Zhao, L., Dai, A. & Dong, B. Changes in global vegetation activity and its driving factors during 1982–2013. *Agric. For. Meteorol.* **249** (2018).
56. Zhang, Y., Song, C., Band, L. E., Sun, G. & Li, J. Reanalysis of global terrestrial vegetation trends from MODIS products: Browning or greening? *Remote Sens. Environ.* **191** (2017).
57. Sari Astuti, I. *et al.* Drought indices to map forest fire risks in topographically complex mountain landscapes. *KnE Soc. Sci.* https://doi.org/10.18502/kss.v7i16.12167 (2022).
58. Wang, H. *et al.* Greening or browning? The macro variation and drivers of different vegetation types on the Qinghai-Tibetan Plateau from 2000 to 2021. *Front. Plant Sci.* **13** (2022).
59. Keeley, J. E. Fire intensity, fire severity and burn severity: A brief review and suggested usage. *Int. J. Wildl. Fire* **18** (2009).
60. Bond, W. J. & Keeley, J. E. Fire as a global 'herbivore': The ecology and evolution of flammable ecosystems. *Trends Ecol. Evol.* https://doi.org/10.1016/j.tree.2005.04.025 (2005).
61. Haryani, G. S., Hidayat & Samir, O. Diversity of fish caught using gill nets in Lake Sentarum, West Kalimantan—Indonesia. *IOP Conf. Ser. Earth Environ. Sci.* **535**, 012037 (2020).
62. Giesen, W. & Anshari, G. Z. Danau Sentarum National Park (Indonesia). in *The Wetland Book* 1841–1850 (Springer Netherlands, 2018). https://doi.org/10.1007/978-94-007-4001-3_44.
63. Ridwansyah, I., Nasahara, K., Nishiyama, C. & Subehi, L. Land use change analysis at sentarum catchment area, West Kalimantan-Indonesia. *Proceedings of the 16th World Lake Conference* 222–231 (2017).
64. Dennis, R. A. *et al.* Fire, people and pixels: Linking social science and remote sensing to understand underlying causes and impacts of fires in Indonesia. *Hum. Ecol.* **33**, 465–504 (2005).
65. Onrizal. Social and environmental issues of Danau Sentarum National Park, West Kalimantan. *Biodiversitas* **6**, 220–223 (2005).
66. IPCC. Climate Change and Land: an IPCC special report. *Climate Change and Land: an IPCC Special Report on climate change, desertification, land degradation, sustainable land management, food security, and greenhouse gas fluxes in terrestrial ecosystems* (2019).
67. Yu, M., Wang, G. & Chen, H. Quantifying the impacts of land surface schemes and dynamic vegetation on the model dependency of projected changes in surface energy and water budgets. *J. Adv. Model. Earth Syst.* **8**, 370–386 (2016).
68. Wu, M. *et al.* Vegetation–climate feedbacks modulate rainfall patterns in Africa under future climate change. *Earth Syst. Dyn.* **7**, 627–647 (2016).
69. Port, U., Brovkin, V. & Claussen, M. The influence of vegetation dynamics on anthropogenic climate change. *Earth Syst. Dyn.* **3**, 233–243 (2012).
70. Franklin, J., Serra-Diaz, J. M., Syphard, A. D. & Regan, H. M. Global change and terrestrial plant community dynamics. *Proc. Natl. Acad. Sci.* **113**, 3725–3734 (2016).
71. Xu, H., Tan, J., Li, C., Niu, Y. & Wang, J. Exploring the dynamic impact of extreme climate events on vegetation productivity under climate change. *Forests* **14**, 744 (2023).
72. Zhu, L., Sun, S., Li, Y., Liu, X. & Hu, K. Effects of climate change and anthropogenic activity on the vegetation greening in the Liaohe River Basin of northeastern China. *Ecol. Indic.* **148**, 110105 (2023).
73. Lestari, S. *et al.* ENSO influences on rainfall extremes around Sulawesi and Maluku Islands in the Eastern Indonesian Maritime Continent. *SOLA* **12**, 37–41 (2016).
74. Aldrian, E., Dümenil Gates, L. & Widodo, F. H. Seasonal variability of Indonesian rainfall in ECHAM4 simulations and in the reanalyses: The role of ENSO. *Theor. Appl. Climatol.* **87**, 41–59 (2007).
75. Juneng, L. & Tangang, F. T. Evolution of ENSO-related rainfall anomalies in Southeast Asia region and its relationship with atmosphere–ocean variations in Indo-Pacific sector. *Clim. Dyn.* **25**, 337–350 (2005).
76. Supari, *et al.* ENSO modulation of seasonal rainfall and extremes in Indonesia. *Clim. Dyn.* **51**, 2559–2580 (2018).
77. Ng, C. H. J., Vecchi, G. A., Muñoz, Á. G. & Murakami, H. An asymmetric rainfall response to ENSO in East Asia. *Clim. Dyn.* **52** (2019).
78. Thouret, J. C. *et al.* Semeru volcano, Indonesia: measuring hazard, exposure and response of densely populated neighbourhoods facing persistent volcanic threats. *Natl. Hazards* **117** (2023).

79. Thouret, J. C., Lavigne, F., Suwa, H., Sukatja, B. & Surono. Volcanic hazards at Mount Semeru, East Java (Indonesia), with emphasis on lahars. *Bull. Volcanol.* **70** (2007).
80. Hadiwijoyo, E. Pola Kebakaran Hutan di Areal Konservasi Studi Kasus di Taman Nasional Bromo Tengger Semeru Forest Fire Pattern in Conservation Area Case Study in Bromo Tengger Semeru National Park. *Jurnal Silvikultur Tropika* **14** (2023).
81. Aini, N. & Sukojo, B. M. Pemanfaatan Data Landsat-8 dan MODIS untuk Identifikasi Daerah Bekas Terbakar Menggunakan Metode NDVI (Studi Kasus: Kawasan Gunung Bromo). *Jurnal Teknik ITS* **5** (2016).
82. Chazdon, R. L. Beyond deforestation: Restoring forests and ecosystem services on degraded lands. *Science* https://doi.org/10.1126/science.1155365 (2008).
83. Le, H. D., Smith, C. & Herbohn, J. What drives the success of reforestation projects in tropical developing countries? The case of the Philippines. *Glob. Environ. Change* **24** (2014).
84. Le, H. D., Smith, C., Herbohn, J. & Harrison, S. More than just trees: Assessing reforestation success in tropical developing countries. *J. Rural Stud.* https://doi.org/10.1016/j.jrurstud.2011.07.006 (2012).
85. Yang, Y. *et al.* Large ecosystem service benefits of assisted natural regeneration. *J. Geophys. Res. Biogeosci.* **123**, 676–687 (2018).
86. Bruner, A. G., Gullison, R. E., Rice, R. E. & Da Fonseca, G. A. B. Effectiveness of parks in protecting tropical biodiversity. *Science (1979)* **291** (2001).

Author contributions

F.R: Conceptualization, Methodology, Data Processing using GEE, Formal Analysis, Visualization, Writing—Original Draft. P.S: Literatures Review, Formal Analysis, Visualization, Writing—Review & Editing. R.S: Data Processing using GEE, Investigation, Writing—Review & Editing, Visualization.

Competing interests

The authors declare no competing interests.

Additional information

Correspondence and requests for materials should be addressed to F.R.

Reprints and permissions information is available at www.nature.com/reprints.

Publisher's note Springer Nature remains neutral with regard to jurisdictional claims in published maps and institutional affiliations.